Robust Control of Maglev Vehicles with Multimagnets Using Separate Control Techniques

Jeon Soo Park*
School of Computer-Aided Design, Daeduk College, Taejeon 305-715, Korea
Jong Shik Kim, Jin Kul Lee
School of Mech. Eng., Pusan National University 30 Changjeon-dong, Kumjeong-gu, Pusan 609-735, Korea

A robust control design scheme using well-developed SISO techniques is proposed for maglev vehicles that are inherently unstable MIMO systems. The proposed seperate control method has basically two control loops: a stabilizing loop by a pole-placement technique, and a performance loop using a novel optimal LQ loop-shaping technique. This paper shows that the coupling terms involved in maglev vehicles with multimagnets should not be neglected but compensated for their stability and performance robustness. The robustness properties of the proposed control system are then evaluated under variations of vehicle masses and air gaps through a computer simulation. This paper also describes the reason why the proposed control technique can be suggested as a tool using only SISO techniques in controlling unstable MIMO systems such as maglev vehicles.

Key Words: Maglev Vehicle, Robustness, Loop-Shaping, Coupling Effect, Separate Control Technique

Nomenclature

f_i : Magnetic force in the i^{th} corner of maglev vehicles
z_i : Air gap in the i^{th} corner of maglev vehicles
z_g, z_θ, and z_ϕ : Air gaps with respect to heave, pitch, and roll
$\ddot{z}$, $\ddot{\theta}$, and $\ddot{\phi}$: Accelerations with respect to heave, pitch, and roll
F_Z : Total magnetic force for heave direction
T_θ : Torque for pitch direction
T_ρ : Torque for roll direction
M : Total mass of maglev vehicles
I_θ and I_ϕ : Inertial moments about pitch and roll axes
l and b : Half length and width of maglev vehicles
K_z : Circuit constant with respect to air gap
K_I : Circuit constant with respect to current
R_i : Resistance of the i^{th} circuit transducer
N : Number of turns
z_0, y_0, and I_0 : Nominal values with respect to heave, guidance, and current
$|C_{\ddot{v}}|$: Coupling matrix of maglev vehicles
$\{f_{ext}(t)\}$: Disturbance vector
$A_{\ddot{u}}$: System matrix for local control system
$A_{\ddot{v}}$: System matrix imposed by coupling terms
b_i : Input vector
Γ_i : Disturbance input matrix
$u_i^l(t)$: Local control law
$u_i^c(t)$: Complementary control law
$u_p(t)$: Actual control law for a given

* Corresponding Author,
E-mail : jspark@mail.ddc.ac.kr
TEL : +82-42-866-0387; **FAX** : +82-42-444-6670
School of Computer-Aided Design, Daeduk College, Taejeon 305-715, Korea. (Manuscript **Received** December 22, 2000; **Revised** June 13, 2001)

plant

G : Optimal LQ loop-shaping control gain

K : Pole-placement control gain

L : Loop-shaping design parameter

ρ : Scaling design parameter

$G_F(s)$: Loop transfer function for a given plant

$\Phi(s)$: State transition function for a given plant

1. Introduction

In recent years, many researchers have reported on magnetically levitated (maglev) systems with their own conclusions and suggestions, and they are likely to have made a great jump in the modeling (Limbert, 1979; Sinha, 1987) and control (Fabien, 1993; MacLeod and Goodall, 1996) of maglev systems. However, studies so far performed are chiefly related to a 1-DOF (degree of freedom) system. They have assumed the maglev's dynamic behavior to be in only one direction (heave motion), or in more complicated analyses, a two-directional model including both heave and lateral motions but with the model separated along each DOF, neglecting the coupling effects between the two DOFs.

Maglev vehicles, in general, contain six DOFs, which correspond to the three rectilinear motions- the heave, lateral, and propulsion motions by their respective drivers, and to the three rotational motions - the yawing, pitching, and rolling motions by their own rigid-body behavior. The vehicle studied in this paper is the most commonly chosen model in EMS (electromagnetic suspension), which uses linear motors to produce the propulsion force and electromagnets to generate the heave and lateral forces. In EMS, unlike in EDS (electrodynamic suspension) which operates at relatively stable states by using a repulsive force proportional to the vehicle's velocity, the attractive forces in the heave and lateral directions are inversely proportional to the air gaps, so that the vehicle must require some control circuits to give stability and to guarantee safety and ride quality as a usual criteria for passenger transporting systems.

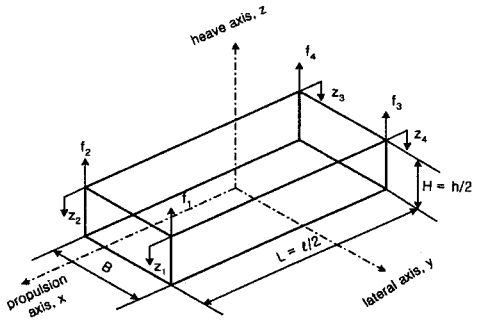

Fig. 1 Schematic diagram of maglev vehicles with multimagnets

We attempt to analyze and design for the heave model of maglev vehicles in EMS, with the intention that dynamic models of a system may give different responses with respect to whether or not it is considered full-scale in space. First, maglev vehicles viewed as a rigid body are modeled by taking all motions (one rectilinear and two rotational motions) into account, and simple decoupling concepts are effectively discussed for controlling a multivariable maglev system having 4 inputs and 4 outputs. Second, an optimal loop-shaping LQ technique (Kim, 1987) is briefly introduced and applied for each of the decoupled systems, and a total control law capable of compensating for the neglected terms is designed. Finally, the stability and performance for the suggested maglev control system are evaluated under the variation of air gaps and vehicle masses through a computer simulation.

2. Modeling of Maglev Vehicles

Figure 1 shows the schematic model for one full car, that is not a simple one magnet, of a maglev vehicle considered in this paper, where electromagnets for suspension forces are attached at each corner of the car. In Fig. 1, $f_i(i=1$ to $4)$ denote the suspension forces, and $z_i(i=1$ to $4)$ are the air gaps measured downwards from the arbitrarily fixed datum.

Maglev vehicles like Fig. 1 normally have three major components that are directly related to each coordinate axis: the propulsion, guidance, and

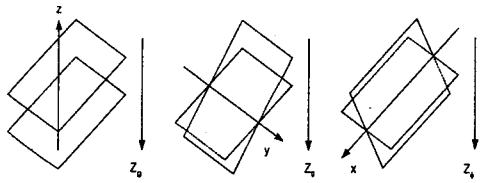

(a) Heave (b) Pitch (c) Roll

Fig. 2 Possible motions for heave direction

suspension devices. Since it is possible, in practice, to operate them independently, we here focus only on modeling the dynamics reflected to the heave axis. Thus, the selected motions can be reduced to those in Fig. 2, which include one rectilinear motion along the heave axis and two rotational motions about the pitch and roll axes.

In Fig. 2, z_g, z_θ and z_ϕ denote the displacements projected onto the heave direction by all rigid-body motions. For small perturbations around the nominal operating points in the suspension z, pitch θ and roll ϕ, the equations of motion can be expressed in a matrix form as

$$\begin{Bmatrix} F_z \\ T_\theta \\ T_\phi \end{Bmatrix} = \begin{bmatrix} M & 0 & 0 \\ 0 & I_\theta & 0 \\ 0 & 0 & I_\phi \end{bmatrix} \begin{Bmatrix} \ddot{z} \\ \ddot{\theta} \\ \ddot{\phi} \end{Bmatrix} \tag{1}$$

where F_z, T_θ and T_ϕ are the sum of the suspension forces and the sums of the rotational torques generated by the pitch and roll movements, and M, I_θ and I_ϕ are the total mass of vehicle and the inertia moments about the pitch and roll axes, respectively. Eq. (1) describes a general form for vehicle dynamics in space, so that when using actual geometric relations it must be transformed into a more specialized version that can be easily utilized in the application domain. The relation between the excitations in Eq. (1) and actual magnetic forces, and the relation between the motion variables in Eq. (1) and actual measurable variables are as follows:

$$\begin{bmatrix} 1 & 0 & 0 \\ 0 & 1/2l & 0 \\ 0 & 0 & 1/2b \end{bmatrix} \begin{Bmatrix} F_z \\ T_\theta \\ T_\phi \end{Bmatrix} = \begin{bmatrix} 1 & 1 & 1 & 1 \\ -1 & -1 & 1 & 1 \\ 1 & -1 & 1 & -1 \end{bmatrix} \begin{Bmatrix} f_1 \\ f_2 \\ f_3 \\ f_4 \end{Bmatrix} \tag{2}$$

$$\begin{Bmatrix} z_1 \\ z_2 \\ z_3 \\ z_4 \end{Bmatrix} = \begin{bmatrix} -1 & l & -b \\ -1 & l & b \\ -1 & -l & -b \\ -1 & -l & b \end{bmatrix} \begin{Bmatrix} z \\ \theta \\ \phi \end{Bmatrix} \tag{3}$$

where l and b are, respectively, the half length and half width of the car calibrated from the centers to the sensors at each corner. We now use the well-known result for the magnet forces in Eq. (2), which was originally derived under the situation that a certain staggered configuration of magnets produces suspension forces f_i in both the heave and lateral directions, but the forces can be easily decoupled into each direction by choosing the sum and difference of input voltages in the magnet transducer as new input variables (Limbert, 1979; Kim and Park, 1991). Applying Taylor's series, the linearized governing equations for the heave direction are as follows:

$$f_i(t) = K_z z_i(t) - K_I I_i(t) \tag{4}$$

$$v_i(t) = R_i I_i(t) + L_0 \dot{I}_i(t) - 2 I_0 L_z \dot{z}_i(t) \tag{5}$$

where R_i are the resistances of each magnet driver, and the coefficients associated with the air gap and current K_z and K_I, the nominal inductance L_0, and the inductance L_z per unit length are respectively given by

$$K_z = \mu_0 A N^2 \left(\frac{I_0}{z_0}\right)^3 \left(\frac{2\alpha_0 - \alpha_1}{I_0}\right),$$

$$K_I = \mu_0 A N^2 \left(\frac{I_0}{z_0}\right)^2 \left(\frac{\alpha_0}{I_0}\right),$$

$$L_0 = \frac{\mu_0 A N^2}{2 z_0} \left(1 - \kappa_r \frac{y_0}{w}\right),$$

$$L_z = \frac{\mu_0 A N^2}{2 z_0^2} \left(1 - \kappa_r \frac{y_0}{w}\right).$$

where

$$\alpha_0 = 1 + \frac{2 z_0}{\pi w} \tan^{-1} \frac{y_0}{z_0}, \quad \alpha_1 = \frac{2 z_0}{\pi w} \left(1 + \frac{y_0^2}{z_0^2 + y_0^2}\right),$$

and μ_0 is the permeability of free space; N is the number of turns; A is the cross-sectional area of the magnet at each corner of the car, which is the product of the width w and length p of the magnet; κ_r is a compensation factor that makes the analytical model for magnetic flux flow more realistic, and is usually between $-w/y_0$ and w/y_0; finally, (z_0, y_0, I_0) denotes the nominal values of the vertical and lateral air gaps and the current, respectively, at the operating point.

Figure 3 shows the block diagram of the maglev system presented in this paper, which can be considered as a 4-input and 4-output multivariable system that contains mutual

interference due to geometric constraints. However, the constraints are represented only by the vehicle parameters, so that we can think of the model between the magnet forces and absolute accelerations as a sort of transformation device whose behavior shows no dynamic characteristics at all. This idea can give a more simple method for dealing with a complicated system such as Fig. 3, that is, a separate control method that enables us to control MIMO systems (called global terms in this sense) with a well-developed SISO technique by separating them into the local terms having only channel-to-channel relations, and the coupling terms having the effect for one channel to contribute to the others' channels. From Fig. 3, the coupling terms c_{ij} from the i^{th} input channel to the j^{th} output channel can be calculated as a function of only the geometric parameters by

$$[C_{ij}]=\begin{bmatrix} 1 & -l & -b \\ 1 & -l & b \\ 1 & l & -b \\ 1 & l & b \end{bmatrix}\begin{bmatrix} 1/M_z & 0 & 0 \\ 0 & 1/T_\theta & 0 \\ 0 & 0 & 1/T_\phi \end{bmatrix}\begin{bmatrix} 1 & 1 & 1 & 1 \\ -l/2 & -l/2 & l/2 & l/2 \\ -b/2 & b/2 & -b/2 & b/2 \end{bmatrix} \tag{6}$$

With Eq. (3), the global governing equations including the local and coupling terms are then represented in matrix-vector form as follows:

$$\{\ddot{z}(t)\}=[C_{ij}][K_z]\{z(t)\}-[K_I]\{i(t)\}+[D_{ij}]\{f_{ext}(t)\} \tag{7}$$

where $\{\bullet\}$ denotes vectors whose elements are the corresponding quantities at each corner of the maglev system, except for the last term $\{f_{ext}(t)\}$ which is a disturbance vector unreasonably excited along each motion of the maglev system, and

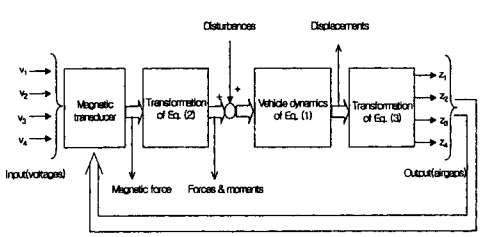

Fig. 3 Block diagram of maglev vehicles

$[\bullet]$ denotes matrices where $[K_z]$ and $[K_I]$, in particular, are diagonal matrices consisting of the circuit coefficients at each corner of the maglev system.

3. Controller Design of Maglev Vehicles

We now try to seek an effective control law for a MIMO maglev system. This method will adopt appropriate SISO techniques and make us avoid the effort to find a new and complex method for MIMO systems. From Eq. (7), the state space model of the i^{th} subsystem can be described as

$$\dot{x}_i(t)=A_{ii}x_i(t)+\sum_{j=1,j\neq i}A_{ij}x_j(t)+b_iu_i(t)+\Gamma_i d_i(t) \tag{8}$$

where the state vector $x_i(t)$ is $[z_i(t)\dot{z}_i(t)i_i(t)]^T$; the control input vector $u_i(t)$ is the voltage on each magnetic circuit; the disturbance vector $d_i(t)$ is $[f_{ext}^z f_{ext}^\theta f_{ext}^\phi]^T$ whose elements are external signals exerted along the directions of heave, pitch, and roll.

Equation (8) shows one of the ways in which the global system of Eq. (7) can be separated into systems involving both the local and coupling terms as mentioned in the early section. The local term A_{ii} in Eq. (8) denotes the system matrix involving only the corner-to-corner effect in which the interactions between different corners of the maglev vehicle are neglected, while the coupling term $A_{ij}(j\neq i)$ indicates the influence of the j^{th} input on the i^{th} output, and may be seen as a complementary matrix that makes the local term become a global system. The terms involved in Eq. (8) are as follows:

$$A_{ii}=\begin{bmatrix} 0 & 1 & 0 \\ C_{ii}K_z/M_z & 0 & -C_{ii}K_i/M_z \\ 0 & 2I_0L_z/L_0 & -R/L_0 \end{bmatrix}\quad b_i=\begin{bmatrix} 0 \\ 0 \\ 1/L_0 \end{bmatrix}$$

$$A_{ij}=\begin{bmatrix} 0 & 0 & 0 \\ C_{ij}K_z & 0 & -C_{ij}K_i \\ 0 & 0 & 0 \end{bmatrix}\quad \Gamma_i=\begin{bmatrix} 0 & 0 & 0 \\ D_{i1} & D_{i2} & D_{i3} \\ 0 & 0 & 0 \end{bmatrix}$$

where Γ_i is the disturbance matrix whose elements $D_{ij}(j=1,2,3)$ have no mathematical description now, but can be easily calculated if needed as in

cases when more accurate disturbances like rail irregularities and track deflection should be considered.

On the other hand, it is necessary to decouple the C_{ij} involved in each term of Eq. (8), so that a well-defined SISO technique can be applied to control the MIMO maglev vehicles without any modification. Note that the coupling term of Eq. (6) has the properties that $C_{ij}=C_{ji}$ (symmetric matrix) and its diagonal elements are all equal to each other. Then Eq. (8) can be easily transformed into the following state space model with the constant system matrix regardless of the subscript. That is,

$$\dot{x}_i(t)=A_0x_i(t)+\sum_{j=1}^{4}A_{ij}x_j(t)+b_iu_i(t)+\Gamma_id_i(t) \quad (9)$$

where

$$A_0=\begin{bmatrix} 0 & 1 & 0 \\ K_z/M_z & 0 & -K_i/M_z \\ 0 & 2I_0L_z/L_0 & -R/L_0 \end{bmatrix}$$

$$A_{ij}=\begin{bmatrix} 0 & 0 & 0 \\ C_{ij}K_z & 0 & -C_{ij}K_i \\ 0 & 0 & 0 \end{bmatrix} \quad (i\neq j)$$

$$A_{ij}=\begin{bmatrix} 0 & 0 & 0 \\ \beta K_z & 0 & -\beta K_z \\ 0 & 0 & 0 \end{bmatrix} \quad (i=j)$$

$$\beta=\frac{(l/2)^2}{2I_\theta}+\frac{(b/2)^2}{2I_\phi}$$

3.1 Construction of separate control systems

Comparing Eq. (9) with the state space model of most frequently used maglev systems that are generally assumed to have a single magnet and are characterized as a SISO system, it can be seen that the only difference is whether or not the coupling term A_{ij} exists. Thus, the decoupced control scheme presented in this paper can be rather easily implemented just by incorporating the A_{ij} into the local term as a whole.

Applying such an idea to Eq. (9), the reconstructed model is given as

$$\dot{x}_i(t)=A_0x_i(t)+bu_i^l(t) \quad (10)$$

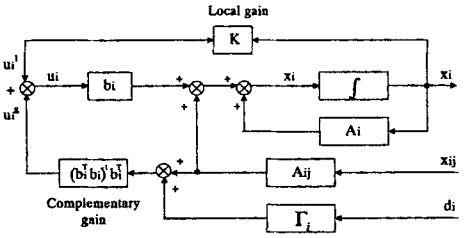

Fig. 4 Structure of separate control systems

where u_i^l is the local control which can be thought of as that for a SISO maglev system, and its relation to the actual control $u_i(t)$ in the global sense is simply as follows:

$$b_iu_i^l(t)=b_iu_i(t)+\sum_{j=1}^{4}A_{ij}x_j(t)+\Gamma_id_i(t) \quad (11)$$

Equation (10) shows that a MIMO maglev vehicle can be controlled by designing the controls for each corner separately, in which case the coupling terms are regarded as externally disturbing inputs. If we can select only the local control $u_i^l(t)$ to meet the required robustness of stability and performance using a well-developed SISO technique, the actual (global) control that can compensate for the coupling effects A_{ij} becomes

$$u_i(t)=u_i^l(t)+u_i^c(t) \quad (12)$$

where $u_i^c(t)$ is a complementary control which indicates the control law only for the coupling terms A_{ij} neglected in designing the local control, From Eq. (11) its mathematical form can be derived by

$$u_i^c(t)=-(b_i^Tb_i)^{-1}b_i^T\left[\sum_{j=1}^{4}A_{ij}x_j(t)+\Gamma_id_i(t)\right] \quad (13)$$

Hence, it is concluded that we can control maglev vehicles like Fig. 1 by constructing a separate control system like Fig. 4. In Fig. 4, the $u_i^l(t)$ plays a role of ensuring the stability and performance robustness required for the control system, while the $u_i^c(t)$ contributes to maintaining a reasonable attitude for the vehicle body in space.

3.2 Local control design

In this paper, the combined pole-placement and optimal loop-shaping LQ technique is

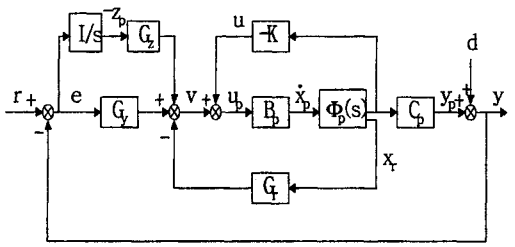

Fig. 5 Structure of the proposed control system

proposed for designing the local control $u_i^l(t)$, where the former is for stabilizing the control system and the latter for improving its performance such as command-following, disturbance rejection, etc. Figure 5 shows the structure of the proposed local control system for a given plant described as

$$\begin{cases}\dot{x}_p(t)=A_p x_p(t)+B_p u_p(t)\\ y_p(t)=C_p x_p(t)\end{cases} \tag{14}$$

where $x_p(t)$, $u_p(t)$, and $y_p(t)$ are the open-loop state, control input, and output variables, respectively.

In Fig. 5, one design parameter K is the stabilizing gain to be selected by pole-placement techniques, and the other parameter $G=|\,G_z\,\vdots\,G_y\,\vdots\,G_r\,|$ is the performance-enhancing gain to be designed by optimal loop-shaping LQ techniques. Also, an integrator is augmented at each error signal for making the control system have zero error in its steady-state response to constant command and disturbance inputs. Thus, the closed-loop state variables of Fig. 5 consist of the augmented state $z_p(t)$, the output of the integrator, the plant output $y_p(t)$, and the remaining state made by eliminating from the original state. With the redefined state vector $x(t)=[z_p(t)\,\vdots\,y_p(t)\,\vdots\,x_r(t)]^T$, the $u(t)$ for the stabilizing loop, the $v(t)$ for the performance loop, and the combined control $u_p(t)$ (equal to the local control $u_i^l(t)$ mentioned in the previous section) of the proposed control system are as follows:

$$u(t)=-Kx_p(t) \tag{15}$$

$$v(t)=-Gx(t)+G_y[r(t)-d(t)] \tag{16}$$

$$u_p(t)=u(t)+v(t) \tag{17}$$

We now discuss briefly the control techniques used in this paper. For the pole-placement control gain K, it is obtained by locating the poles of (A_p-B_pK) at some stable positions in the s-plane. For the optimal loop-shaping gain G, however, more explanation is in order of its advantages over the classical LQ optimal control technique (Bryson, 1975; Doyle and Stein, 1981) in the procedure of finding design parameters, especially for a SISO system.

The optimal loop-shaping technique is based on the systematic selection of the design parameter L satisfying the following frequency-domain equality equation (Kim, 1987)

$$G_F(s)\approx\frac{1}{\sqrt{\rho}}C(sI-A)^{-1}L \tag{18}$$

where $G_F(s)=G\Phi(s)B$ is the target loop transfer function of a given plant with $\Phi(s)=(sI-A)^{-1}$, and G is the optimal loop gain we are to select, once the design parameters have been all chosen, as

$$G=\frac{1}{\rho}B^TP \tag{19}$$

where P is the solution of the following algebraic Riccati equation:

$$PA+A^TP+L^TL-\frac{1}{\rho}PBB_TP=0 \tag{20}$$

In Eq. (18), the ρ is the scaling parameter which can be picked out by adjusting the resultant magnitude of $C(sI-A)^{-1}$ up and down to meet the required cross-over frequency or performance criteria, and the loop-shaping parameter L is used to make the target transfer function formed as a desirable loop shape which usually has a type of pure integrators. For a SISO system, the parameter L can be systematically designed with the idea that the zero polynomial of $G_F(s)$ is the linear combination of n independent (constituent) zero polynomials that can be obtained by sequentially setting each element of L to 1 and keeping the others 0. Note that the L is an $(n\times 1)$ column vector and its n elements can be all used as design parameters independently. Then, we can derive the useful equation related to L as

$$Z_CL=z_d \tag{21}$$

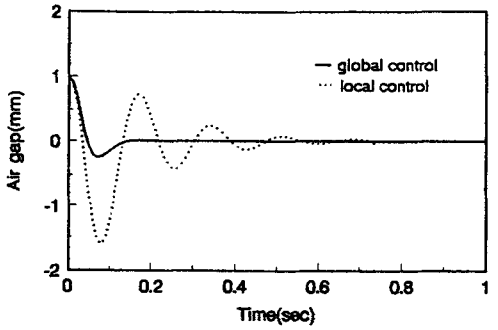

Fig. 6 Step responses of air gap for the global/local control systems

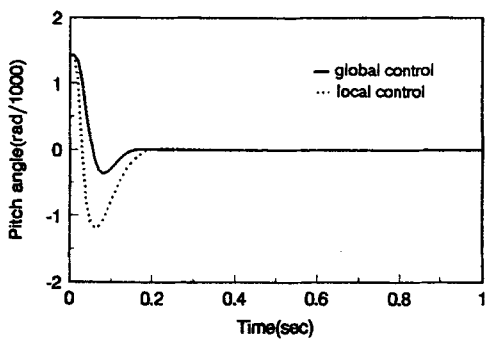

Fig. 7 Step responses of pitch angle for the global/local control systems

where Z_C is the (n×n) matrix containing as its column the coefficients of the constituent zero polynomials of $G_F(s)$, which is generated by successively setting each one of the elements of L to 1 and the others to 0, and then calculating the transfer function for each case; z_d is the desired zero polynomial which can cause the unwanted plant dynamics except the augmented free integrator to be eliminated for all frequencies.

4. Analysis of the Proposed Control System

One of essential performance criteria for maglev vehicles that must be analyzed is the disturbance-rejection performance, which can tell us the degree of regulation against unexpected external inputs such as track irregularities, rail roughness, wind gusts, load variations, and so on. In this paper, we thus confine our attention only to such performances. The effect of the neglected coupling terms on the global system is analyzed for the proposed control system, and its robustness is also evaluated by varying system parameters like vehicle masses and air gaps.

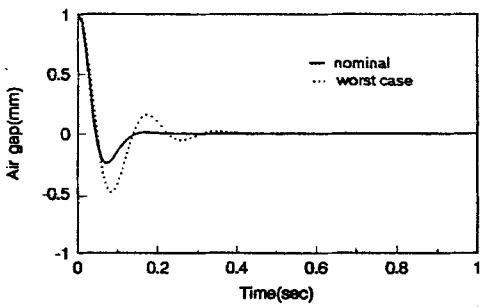

Fig. 8 Nominal and worst-case responses of air gap

Figures 6~7 show the responses of the air gap and pitch angle for the proposed control system against a unit disturbance input, respectively. It can be easily found in Fig. 6 that the local control system without compensating the coupling terms has not only large overshoot but also rapid oscillation when compared with the global control system in which the coupling terms are taken into account. This means that maglev vehicles cannot be modeled as a single magnet, for in such cases, it does not provide enough performance to guarantee stability-robustness and the quality of ride comfort if the coupling terms are not compensated for in a reasonable manner. In Fig. 7, we can see that the pitch movement of the local control system has about two times the magnitude of the global control system. This also means the local control system will have poor safety and reliability.

Figures 8~9 show the nominal and worst responses of the air gap and pitch angle for the proposed control system, respectively, under the assumption that both the vehicle mass and air gap can be varied to ±40%. Here, the worst cases are estimated through several computer simulations to have 40% variation in the mass and -30% in the air gap. In Fig. 8, it is found that the air gap response in the worst case has about 45% overshoot over the operating point but a relatively short settling time of 0. 35 (sec). However, it may be seen that these properties have the ability

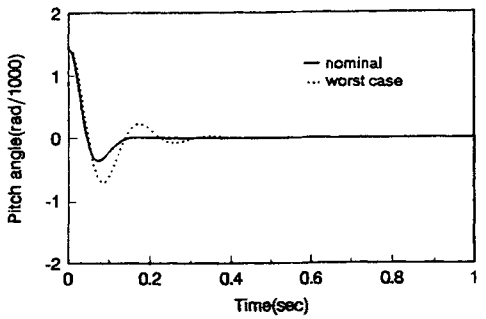

Fig. 9 Nominal and worst-case responses of pitch angle

to maintain the stability and performance robustness to some extent for such relatively large variations of vehicle masses and air gaps. Figure 9 can also be explained as above.

5. Conclusions

A method for controlling MIMO systems by a well-developed SISO technique has been proposed through an example of a maglev vehicle that can be inherently characterized as an unstable MIMO system. The method is a type of separate control methodology, and in this paper consists of a pole-placement technique for stabilizing the unstable control system and an optimal LQ loop-shaping technique for improving its performance, especially disturbance -rejection performance. In addition, in the course of stating the idea behind the decoupled control method, the cross-coupling terms are described mathematically and geometrically in terms of the maglev vehicle parameters. It is found that these effects are essential for ensuring the required specifications, so that they cannot be regarded as external disturbances directly in the modeling process.

Finally, the stability and performance robustness of the proposed control system are evaluated by computer simulation. It is also shown that the proposed system meets such robustness requirement to a reasonable degree in spite of the parameter variations of the vehicle masses and air gaps. Thus, the proposed technique can be suggested as a tool using only SISO techniques in controlling unstable MIMO systems such as maglev vehicles.

References

Bryson, A. E. and Ho, Y. C., 1975, *Applied Optimal Control*, Hemisphere Pub. Co.

Doyle, J. C. and Stein, G., 1981, "Multivariable Feedback Design: Concepts for a Classical/ Modern Synthesis," *IEEE Trans. on AC*, Vol. 26, pp. 4~16.

Fabien, B. C., 1993, "Controller Gain Selection for an Electromagnetic Suspension Under Random Excitation," *ASME J. of Dyn. Sys. Meas. and Control*, Vol. 115, pp. 156~165.

Fallside, F., 1977, *Control System Design by Pole-Zero Assignment*, Academic Press.

Kim, J. S., 1987, "Nonlinear Multivariable Control Using Statistical Linearization and Loop Transfer Recovery," Ph. D. Thesis, Dept of Mech. Eng., MIT.

Lehtomaki, N. A., 1981, "Practical Robustness Measures in Multivariable Control System Analysis," Ph. D. Thesis, Dept. of EECS, MIT.

Limbert, D. A., Richardson, H. H., and Wormley, D. N., 1979, "Controlled Dynamic Characteristics of Ferromagnetic Vehicle Suspension Providing Simultaneous Lift and Guidance," *ASME J. of Dyn. Sys. Meas. and Control*, pp. 217~222.

Kim, J. S. and Park, J. S., 1991, "Bond Graph Modeling and LQG/LTR Controller Design of Magnetically Levitation Systems," *Trans. of KSME*, Vol. 15, pp. 1620~1634.

MacLeod, C. and Goodall, R. M., 1996, "Frequency-Shaping LQ Control of Maglev Suspension Systems for Optimal Performance with Deterministic and Stochastic Inputs," *IEEE Proc. on Control Theory Appl.*, Vol. 143, pp. 25~30.

Sinha, P. K., 1987, *Electromagnetic Suspension: Dynamic and Control*, Peter Peregrinus Ltd.